Structural Engineering and Mechanics, *Vol. 66, No. 1 (2018) 61-73*
DOI: https://doi.org/10.12989/sem.2018.66.1.061

Improved HSDT accounting for effect of thickness stretching in advanced composite plates

Abdelhakim Bouhadra[1, 2], Abdelouahed Tounsi*[1, 3], Abdelmoumen Anis Bousahla[1, 4, 5], Samir Benyoucef[1] and S.R. Mahmoud[6]

[1]*Materials and Hydrology Laboratory, University of Sidi Bel Abbes, Faculty of Technology, civil Engineering Department, Algeria*
[2]*Université de Abbés Laghrour Khenchela, Faculté de Sciences & Technologie, Département de Génie Civil, Algeria*
[3]*Department of Civil and Environmental Engineering, King Fahd University of Petroleum & Minerals, 31261 Dhahran, Eastern Province, Saudi Arabia*
[4]*Laboratoire de Modélisation et Simulation Multi-échelle, Université de Sidi Bel Abbés, Algeria*
[5]*Centre Universitaire de Relizane, Algérie*
[6]*Department of Mathematics, Faculty of Science, King Abdulaziz University, Jeddah, Saudi Arabia*

(Received November 21, 2017, Revised January 28, 2018, Accepted January 29, 2018)

Abstract. In this article, a higher shear deformation theory (HSDT) is improved to consider the influence of thickness stretching in functionally graded (FG) plates. The proposed HSDT has fewer numbers of variables and equations of motion than the first-order shear deformation theory (FSDT), but considers the transverse shear deformation influences without requiring shear correction coefficients. The kinematic of the present improved HSDT is modified by considering undetermined integral terms in in-plane displacements and a parabolic distribution of the vertical displacement within the thickness, and consequently, the thickness stretching influence is taken into account. Analytical solutions of simply supported FG plates are found, and the computed results are compared with 3D solutions and those generated by other HSDTs. Verification examples demonstrate that the developed theory is not only more accurate than the refined plate theory, but also comparable with the HSDTs which use more number of variables.

Keywords: functionally graded plates; bending; vibration; computational modeling

1. Introduction

The concept of functionally graded materials (FGMs) was initially proposed in 1984 by scientists in Japan (Koizumi 1997). FGM is a type of composite materials that presents continuous distribution of material characteristics from one surface to another and hence eliminates the concentration of stress encountered in laminated structures. Generally, the FGM is fabricated with a mixture of a metal and a ceramic. FGMs are widely employed in different structural applications such as aerospace, mechanical, civil, and automotive (Zine *et al.* 2018, Meksi *et al.* 2018, Attia *et al.* 2018, Sekkal *et al.* 2017a, Barati and Shahverdi 2016, Bousahla *et al.* 2016, Kar *et al.* 2016, Ahouel *et al.* 2016, Hadji *et al.* 2015, Larbi Chaht *et al.* 2015, Zidi *et al.* 2014, Bouderba *et al.* 2013). When the use of FGMs increases, more accurate models are required to predict their behaviors.

Since the shear deformation influences are more found in thicker plates or plates fabricated from FGMs, shear deformation models like FSDT (Al-Basyouni *et al.* 2015) and HSDTs should be utilized to investigate FG plates. The FSDT provides acceptable numerical results, but use a shear correction coefficient (Mousavi and Tahani 2012, Malekzadeh and Monajjemzadeh 2013, Bouderba *et al.* 2016, Bellifa *et al.* 2016, Arani and Kolahchi 2016, Beldjelili *et al.* 2016, Kolahchi *et al.* 2016b, Madani *et al.* 2016, Zamanian *et al.* 2017, Kolahchi *et al.* 2017a, Zarei *et al.* 2017, Shokravi 2017a).

Whereas, the HSDTs (Touratier 1991, Soldatos 1992, Redd 2000, Karama *et al.* 2003, Zenkour 2006, Pradyumna and Bandyopadhyay 2008, Mantari and Guedes Soares 2012, Thai and Kim 2013, Ahmed 2014, Kar and Panda 2016, Mahapatra *et al.* 2016, Akavci 2016, Kolahchi *et al.* 2016a, Bilouei *et al.* 2016, Baseri *et al.* 2016, Hachemi *et al.* 2017, Klouche *et al.* 2017, Kolahchi and Cheraghbak 2017, Kolahchi 2017, Shokravi 2017b, c, d, Kolahchi and Bidgoli 2016, Houari *et al.* 2016, Boukhari *et al.* 2016, Bellifa *et al.* 2017a, b, Benadouda *et al.* 2017, Zidi *et al.* 2017, Kolahchi *et al.* 2017b, c, Hajmohammad *et al.* 2017, Bakhadda *et al.* 2018) do not employ a shear correction coefficient, but their governing equations are more difficult than those generated by the FSDT. Recently, novel plate models, which consider only four unknown variables and yet take into consideration shear deformations, are proposed by Tounsi *et al.* (2013), Barati and Shahverdi (2016) and Bounouara *et al.* (2016). These theories are based on the idea of partitioning the vertical displacements into the bending and shear components as is firstly proposed by Huffington (1963), and later adopted by Krishna Murty (1987) and Senthilnathan *et al.* (1987). The thickness stretching effect is recently studied by several researchers

*Corresponding author, Professor
E-mail: tou_abdel@yahoo.com

ISSN: 1225-4568 (Print), 1598-6217 (Online)

for beams and plates structures (Benchohra *et al.* 2018, Abualnour *et al.* 2018, Sekkal *et al.* 2017b, Bouafia *et al.* 2017, Sekkal *et al.* 2017a, Akavci 2016, Bennoun *et al.* 2016, Draiche *et al.* 2016, Bourada *et al.* 2015, Hamidi *et al.* 2015, Belabed *et al.* 2014, Fekrar *et al.* 2014, Bousahla *et al.* 2014, Bessaim *et al.* 2013). However, a new idea is proposed initially by Mantari and Granados (2015) by considering undetermined integral terms in in-plane displacements to construct a new FSDT. This idea is improved recently by Merdaci *et al.* (2016), Besseghier *et al.* (2017), Chikh *et al.* (2017), Khetir *et al.* (2017), Menasria *et al.* (2017) and El-Haina *et al.* (2017) to develop new HSDTs.

The purpose of this work is to improve the theory proposed by Mantari and Granados (2015) by considering the influences of shear deformation and thickness stretching in FG plates. The kinematic of the Mantari and Granados (2015) is modified by assuming a new hyperbolic variation of the vertical displacement within the thickness, and thus, the thickness stretching influence is taken into consideration. Thus, the highlight of this theory is that, in addition to including the thickness stretching effect ($\varepsilon_z \neq 0$), the displacement field is modeled with only 5 unknowns. Analytical solutions for bending and dynamic problems are determined for a simply supported rectangular plate. Numerical examples are presented to check the accuracy of the proposed method.

2. Kinematics

The displacement field of the conventional HSDT is given by (Mahi *et al.* 2015)

$$\begin{aligned} u\left(x,y,z,t\right) &= u_0(x,y,t) - z\,\frac{\partial w_0}{\partial x} + f\left(z\right)\varphi_x(x,y,t) \\ v\left(x,y,z,t\right) &= v_0(x,y,t) - z\,\frac{\partial w_0}{\partial y} + f\left(z\right)\varphi_y(x,y,t) \\ w\left(x,y,z,t\right) &= w_0(x,y,t) \end{aligned} \tag{1}$$

$u_0, v_0, w_0, \phi_x, \phi_y$ Are the five unknown displacement of the mid-plane of the plate. By considering that (Fahsi *et al.* 2017) $\phi_x = \int \theta(x,y,t)\,dx$ and $\phi_y = \int \theta(x,y,t)\,dy$ and taking into account the stretching effect, we will have

$$\begin{aligned} u(x,y,z,t) &= u_0(x,y,t) - z\frac{\partial w_0}{\partial x} + k_1\, f(z)\int \theta(x,y,t)\,dx \\ v(x,y,z,t) &= v_0(x,y,t) - z\frac{\partial w_0}{\partial y} + k_2\, f(z)\int \theta(x,y,t)\,dy \\ w(x,y,z,t) &= w_0(x,y,t) + g(z)\varphi_z(x,y,t) \end{aligned} \tag{2}$$

Where

$$k_1 = \alpha^2, \quad k_2 = \beta^2 \tag{3}$$

The new shape function $f(z)$ is given as follows

$$f(z) = \pi^2 z\left(\sqrt[3]{0.135}\cosh\left(\frac{\pi}{h}z\right) - \pi\right) \tag{4}$$

$$g(z) = \frac{df(z)}{dz} \tag{5}$$

The kinematic relations can be obtained as follows

$$\begin{aligned} \begin{Bmatrix} \varepsilon_x \\ \varepsilon_y \\ \gamma_{xy} \end{Bmatrix} &= \begin{Bmatrix} \varepsilon_x^0 \\ \varepsilon_y^0 \\ \gamma_{xy}^0 \end{Bmatrix} + z\begin{Bmatrix} k_x^b \\ k_y^b \\ k_{xy}^b \end{Bmatrix} + f(z)\begin{Bmatrix} k_x^s \\ k_y^s \\ k_{xy}^s \end{Bmatrix} \\ \begin{Bmatrix} \gamma_{yz} \\ \gamma_{xz} \end{Bmatrix} &= g(z)\begin{Bmatrix} \gamma_{yz}^0 \\ \gamma_{xz}^0 \end{Bmatrix} \\ \varepsilon_z &= g'(z)\,\varepsilon_z^0 \end{aligned} \tag{6}$$

Where

$$\begin{Bmatrix} \varepsilon_x^0 \\ \varepsilon_y^0 \\ \gamma_{xy}^0 \end{Bmatrix} = \begin{Bmatrix} \dfrac{\partial u_0}{\partial x} \\ \dfrac{\partial v_0}{\partial y} \\ \dfrac{\partial u_0}{\partial y} + \dfrac{\partial v_0}{\partial x} \end{Bmatrix}, \quad \begin{Bmatrix} k_x^b \\ k_y^b \\ k_{xy}^b \end{Bmatrix} = \begin{Bmatrix} -\dfrac{\partial^2 w_0}{\partial x^2} \\ -\dfrac{\partial^2 w_0}{\partial y^2} \\ -2\dfrac{\partial^2 w_0}{\partial x \partial y} \end{Bmatrix} \tag{7a}$$

$$\begin{aligned} \begin{Bmatrix} k_x^s \\ k_y^s \\ k_{xy}^s \end{Bmatrix} &= \begin{Bmatrix} k_1\theta \\ k_2\theta \\ k_1\dfrac{\partial}{\partial y}\int \theta\,dx + k_2\dfrac{\partial}{\partial x}\int \theta\,dy \end{Bmatrix} \\ \begin{Bmatrix} \gamma_{yz}^0 \\ \gamma_{xz}^0 \end{Bmatrix} &= \begin{Bmatrix} k_2\int \theta\,dy + \dfrac{\partial \varphi_z}{\partial y} \\ k_1\int \theta\,dx + \dfrac{\partial \varphi_z}{\partial x} \end{Bmatrix} \\ \varepsilon_z^0 &= \varphi_z \end{aligned} \tag{7b}$$

The integrals used in the above equations shall be resolved by a Navier type method and can be given as follows

$$\begin{aligned} \frac{\partial}{\partial y}\int \theta\,dx &= A'\frac{\partial^2 \theta}{\partial x \partial y} \\ \frac{\partial}{\partial x}\int \theta\,dy &= B'\frac{\partial^2 \theta}{\partial x \partial y} \\ \int \theta\,dx &= A'\frac{\partial \theta}{\partial x} \\ \int \theta\,dy &= B'\frac{\partial \theta}{\partial y} \end{aligned} \tag{8a}$$

Where the coefficients A' and B' are expressed according to the type of solution used, in this case via Navier.

Therefore, A', B', k_1 and k_2 are expressed as follows

$$A' = -\frac{1}{\alpha^2},\ B' = -\frac{1}{\beta^2}, k_1 = \alpha^2, k_2 = \beta^2 \tag{8b}$$

Where
e μ and β are used in Eq. (24).

3. Constitutive relations

The linear constitutive relations of a FG plate can be expressed as

$$\begin{Bmatrix} \sigma_x \\ \sigma_y \\ \sigma_z \\ \tau_{xz} \\ \tau_{yz} \\ \tau_{xy} \end{Bmatrix} = \begin{bmatrix} C_{11} & C_{12} & C_{13} & 0 & 0 & 0 \\ C_{12} & C_{22} & C_{23} & 0 & 0 & 0 \\ C_{13} & C_{23} & C_{33} & 0 & 0 & 0 \\ 0 & 0 & 0 & C_{44} & 0 & 0 \\ 0 & 0 & 0 & 0 & C_{55} & 0 \\ 0 & 0 & 0 & 0 & 0 & C_{66} \end{bmatrix} \begin{Bmatrix} \varepsilon_x \\ \varepsilon_y \\ \varepsilon_z \\ \gamma_{xz} \\ \gamma_{yz} \\ \gamma_{xy} \end{Bmatrix} \tag{9}$$

The $C_{ij}(i,j=1, 2, 4, 5, 6)$ expressions in terms of engineering constants are given below

$$C_{ii} = \frac{(1-\nu)\lambda(z)}{\nu}, \quad (i = 1,2,3). \tag{10a}$$

$$C_{ij} = \lambda(z), \qquad (i, j = 1,2,3). \tag{10b}$$

$$C_{ii} = \mu(z), \qquad (i = 4,5,6). \tag{10c}$$

$$\lambda(z) = \frac{E(z)}{(1-2\nu)(1+\nu)}, \tag{10d}$$

$$\mu(z) = \frac{E(z)}{2(1+\nu)}, \tag{10e}$$

4. Equations of motion

Hamilton's principle is used herein to derive the equations of motion. The principle can be stated in analytical form as (Ait Amar Meziane *et al.* 2014, Taibi *et al.* 2015, Zemri *et al.* 2015, Attia *et al.* 2015, Belkorissat *et al.* 2015, Ait Yahia *et al.* 2015, Taibi *et al.* 2015, Mouffoki *et al.* 2017, Abdelaziz *et al.* 2017)

$$0 = \int_0^T (\delta U + \delta V - \delta K)dt \tag{11}$$

Where $\boldsymbol{\delta U}$ is the variation of strain energy; $\boldsymbol{\delta V}$ is the variation of potential energy; $\boldsymbol{\delta K}$ is the variation of kinetic energy.

The variation of strain energy of the plate is calculated by

$$\begin{aligned} \delta U &= \int_{-h/2}^{h/2} \int_A [\sigma_x \delta\varepsilon_x + \sigma_y \delta\varepsilon_y + \sigma_z \delta\varepsilon_z \\ &+ \tau_{xy}\delta\gamma_{xy} + \tau_{yz}\delta\gamma_{yz} + \tau_{xz}\delta\gamma_{xz}]dAdz \\ &= \int_A [N_x \delta\varepsilon_x^0 + N_y \delta\varepsilon_y^0 + N_z \delta\varepsilon_z^0 \\ &+ N_{xy}\delta\gamma_{xy}^0 + M_x^b \delta k_x^b + M_y^b \delta k_y^b \\ &+ M_{xy}^b \delta k_{xy}^b + M_x^s \delta k_x^s + M_y^s \delta k_y^s \\ &+ M_{xy}^s \delta k_{xy}^s + S_{yz}^S \delta\gamma_{yz} + S_{xz}^S \delta\gamma_{xz}]dA = 0 \end{aligned} \tag{12}$$

Where $\boldsymbol{A}$ is the surface; and stress resultants N, M, and S are defined by

$$\begin{Bmatrix} N_x & N_y & N_{xy} \\ M_x^b & M_y^b & M_{xy}^b \\ M_x^s & M_y^s & M_{xy}^s \end{Bmatrix} = \int_{-h/2}^{h/2} (\sigma_x, \sigma_y, \tau_{xy}) \begin{Bmatrix} 1 \\ z \\ f(z) \end{Bmatrix} dz \tag{13a}$$

$$N_z = \int_{-h/2}^{h/2} \sigma_z \ \mathrm{g'(z)}\ dz \tag{13b}$$

$$(S_{xz}^s, S_{yz}^s) = \int_{-h/2}^{h/2} (\tau_{xz}, \tau_{yz})\ \mathrm{g(z)}\ dz \tag{13c}$$

The variation of potential energy of the applied loads can be expressed as

$$\delta V = -\int_A q\delta\ (w_0(x,y,t) + g(z)\varphi_z(x,y,t))dA \tag{14}$$

Where q is the distributed transverse load.

The variation of kinetic energy of the plate can be written as

$$\begin{aligned} \delta K &= \int_{-h/2}^{h/2} \int_A [\dot{u}\delta\dot{u} + \dot{v}\delta\dot{v} + \dot{w}\delta\dot{w}]\ \rho(\mathrm{z})dA\ dz \\ &= \int_A \{I_0[\dot{u}_0\delta\dot{u}_0 + \dot{v}_0\delta\dot{v}_0 + \dot{w}_0\delta\dot{w}_0] \\ &- I_1[\dot{u}_0 \frac{\partial\delta\dot{w}_0}{\partial x} + \dot{v}_0 \frac{\partial\delta\dot{w}_0}{\partial y} + \frac{\partial\dot{w}_0}{\partial x}\delta\dot{u}_0 + \frac{\partial\dot{w}_0}{\partial y}\delta\dot{v}_0] \\ &+ I_2[\frac{\partial\dot{w}_0}{\partial x}\frac{\partial\delta\dot{w}_0}{\partial x} + \frac{\partial\dot{w}_0}{\partial y}\frac{\partial\delta\dot{w}_0}{\partial y}] \\ &- J_1[\dot{u}_0 \frac{\partial\delta\dot{\theta}}{\partial x} + \frac{\partial\dot{\theta}}{\partial x}\delta\dot{u}_0 + \dot{v}_0 \frac{\partial\delta\dot{\theta}}{\partial y} + \frac{\partial\dot{\theta}}{\partial y}\delta\dot{v}_0] \\ &+ J_2[\frac{\partial\dot{w}_0}{\partial x}\frac{\partial\delta\dot{\theta}}{\partial x} + \frac{\partial\dot{\theta}}{\partial x}\frac{\partial\delta\dot{w}_0}{\partial x} + \frac{\partial\dot{w}_0}{\partial y}\frac{\partial\delta\dot{\theta}}{\partial y} + \frac{\partial\dot{\theta}}{\partial y}\frac{\partial\delta\dot{w}_0}{\partial y}] \\ &+ K_2[\frac{\partial\dot{\theta}}{\partial x}\frac{\partial\delta\dot{\theta}}{\partial x} + \frac{\partial\dot{\theta}}{\partial y}\frac{\partial\delta\dot{\theta}}{\partial y}] + J_1^s[\dot{w}_0\delta\dot{\varphi}_z + \dot{\varphi}_z\delta\dot{w}_0] + \\ &K_2^s\dot{\varphi}_z\delta\dot{\varphi}_z\}dA \end{aligned} \tag{15}$$

Where dot-superscript convention indicates the differentiation with respect to the time variable t; and (I_0, I_1, J_1, I_2, J_2, K_2, K_2^s) are mass inertias defined as

$$(I_0, I_1, J_1, J_1^s, I_2, J_2, K_2, K_2^s) = \int_{-h/2}^{h/2} (1, z, f, g, z^2, zf, f^2, g^2)\rho(z)dz \tag{16}$$

Substituting the expressions of δU, δV and δK from Eqs. (12), (14), and (15) into Eq. (11) integrating by parts, and collecting the coefficients of δu_0, δv_0, δw_0, $\delta\theta$, and δf_z, the following equations of motion of the plate are obtained

$$\delta u_0: \quad \frac{\partial N_x}{\partial x}+\frac{\partial N_{xy}}{\partial y} = I_0\ddot{u}_0 - I_1\frac{\partial \ddot{w}_0}{\partial x} - J_1\frac{\partial \ddot{\theta}}{\partial x} \tag{17a}$$

$$\delta v_0: \quad \frac{\partial N_{xy}}{\partial x}+\frac{\partial N_y}{\partial y} = I_0\ddot{v}_0 - I_1\frac{\partial \ddot{w}_0}{\partial y} - J_1\frac{\partial \ddot{\theta}}{\partial y} \tag{17b}$$

$$\delta w_0: \quad \frac{\partial^2 M_x^b}{\partial x^2}+2\frac{\partial^2 M_{xy}^b}{\partial x\partial y}+\frac{\partial^2 M_y^b}{\partial y^2}+q = I_0(\ddot{w}_0+\ddot{\theta}) + I_1\left(\frac{\partial \ddot{u}_0}{\partial x}+\frac{\partial \ddot{v}_0}{\partial y}\right) - I_2\nabla^2\ddot{w}_0 - J_2\ddot{\theta} + J_1^s\ddot{\varphi} \tag{17c}$$

$$\delta\theta: \quad -k_1 M_x^s - k_2 M_y^s - (k_1 A' + k_2 B')\frac{\partial^2 M_{xy}^s}{\partial x\partial y} + k_1 A'\frac{\partial S_{xz}^s}{\partial x} + k_2 B'\frac{\partial S_{yz}^s}{\partial y} + q = I_0(\ddot{w}_0+\ddot{\theta}) + J_1\left(\frac{\partial \ddot{u}_0}{\partial x}+\frac{\partial \ddot{v}_0}{\partial y}\right) - J_2\nabla^2\ddot{w}_0 - K_2\ddot{\theta} + J_1^s\ddot{\varphi} \tag{17d}$$

$$\delta\varphi_z: \quad \frac{\partial S_{xz}^s}{\partial x}+\frac{\partial S_{yz}^s}{\partial y} - N_z = J_1^s(\ddot{w}_0+\ddot{\theta}) + K_2^s\ddot{\varphi} \tag{17e}$$

By substituting Eq. (7) into Eq. (9) and the subsequent results into Eq. (13), the stress resultants are obtained as

$$\begin{Bmatrix} N \\ M^b \\ M^s \end{Bmatrix} = \begin{bmatrix} A & B & B^s \\ B & D & D^s \\ B^s & D^s & H^s \end{bmatrix} \begin{Bmatrix} \varepsilon \\ k^b \\ k^s \end{Bmatrix} + \begin{bmatrix} L \\ L^a \\ R \end{bmatrix} \varepsilon_0^z \tag{18a}$$

$$S = A^s\ \gamma$$

$$N_z = R^a\varphi + L(\varepsilon_x^0+\varepsilon_y^0) + L^a(k_x^b+k_y^b) + R(k_x^s+k_y^s) \tag{18b}$$

Where

$$N = \{N_x, N_y, N_{xy}\},\ M^b = \{M_x^b, M_y^b, M_{xy}^b\},\ M^s = \{M_x^s, M_y^s, M_{xy}^s\} \tag{19a}$$

$$S = \{S_{xz}^s, S_{yz}^s\},\ \gamma = \{\gamma_{xz}, \gamma_{yz}\},\ \mathrm{A}^s = \begin{bmatrix} A_{44}^S & 0 \\ 0 & A_{55}^S \end{bmatrix} \tag{19b}$$

$$\varepsilon = \{\varepsilon_x^0, \varepsilon_y^0, \varepsilon_{xy}^0\},\ k^b = \{k_x^b, k_y^b, k_{xy}^b\},\ k^s = \{k_x^s, k_y^s, k_{xy}^s\} \tag{19c}$$

$$A = \begin{bmatrix} A_{11} & A_{12} & 0 \\ A_{12} & A_{22} & 0 \\ 0 & 0 & A_{66} \end{bmatrix},\ B = \begin{bmatrix} B_{11} & B_{12} & 0 \\ B_{12} & B_{22} & 0 \\ 0 & 0 & B_{66} \end{bmatrix},\ D = \begin{bmatrix} D_{11} & D_{12} & 0 \\ D_{12} & D_{22} & 0 \\ 0 & 0 & D_{66} \end{bmatrix} \tag{20a}$$

$$B^s = \begin{bmatrix} B_{11}^s & B_{12}^s & 0 \\ B_{12}^s & B_{22}^s & 0 \\ 0 & 0 & B_{66}^s \end{bmatrix},\ \mathrm{D}^s = \begin{bmatrix} D_{11}^s & D_{12}^s & 0 \\ D_{12}^s & D_{22}^s & 0 \\ 0 & 0 & D_{66}^s \end{bmatrix},\ \mathrm{H}^s = \begin{bmatrix} H_{11}^s & H_{12}^s & 0 \\ H_{12}^s & H_{22}^s & 0 \\ 0 & 0 & H_{66}^s \end{bmatrix} \tag{20b}$$

$$\begin{Bmatrix} L \\ L^a \\ R \\ R^a \end{Bmatrix} = \int_{-h/2}^{h/2} \lambda(z) \begin{Bmatrix} 1 \\ z \\ f(z) \\ zf(z) \end{Bmatrix} g'(z)dz \tag{20c}$$

$$\begin{Bmatrix} A_{11} & B_{11} & D_{11} & B_{11}^s & D_{11}^s & H_{11}^s \\ A_{12} & B_{12} & D_{12} & B_{12}^s & D_{12}^s & H_{12}^s \\ A_{66} & B_{66} & D_{66} & B_{66}^s & D_{66}^s & H_{66}^s \end{Bmatrix} = \int_{-h/2}^{h/2} \lambda(z)\left[1,\ z,\ z^2,\ f(z),\ zf(z),\ f^2(z)\right] \begin{Bmatrix} \frac{1-\nu}{\nu} \\ 1 \\ \frac{1-2\nu}{2\nu} \end{Bmatrix} dz \tag{20d}$$

$$A_{44}^s = A_{55}^s = \int_{-h/2}^{h/2} \mu(z)\,[g(z)]^2\,dz \tag{20e}$$

$$(A_{22}, B_{22}, D_{22}, B_{22}^s, D_{22}^s, H_{22}^s) = (A_{11}, B_{11}, D_{11}, B_{11}^s, D_{11}^s, H_{11}^s) \tag{20f}$$

By substituting Eq. (18) into Eq. (17), the equations of motion can be expressed in terms of displacements ($\boldsymbol{\delta u_0}$, $\boldsymbol{\delta v_0}$, $\boldsymbol{\delta w_0}$, $\boldsymbol{\delta\theta}$, $\boldsymbol{\delta f_z}$) as

$$\begin{aligned} &A_{11}\frac{\partial^2 u_0}{\partial x^2} + A_{12}\frac{\partial^2 v_0}{\partial x\partial y} + A_{66}\left(\frac{\partial^2 u_0}{\partial y^2}+\frac{\partial^2 v_0}{\partial x\partial y}\right) - B_{11}\frac{\partial^3 w_0}{\partial x^3} \\ &-B_{12}\frac{\partial^3 w_0}{\partial x\partial y^2} - 2B_{66}\frac{\partial^3 w_0}{\partial x\partial y^2} + B_{11}^s A' k_1\frac{\partial^3\theta}{\partial x^3} \\ &B_{12}^s B' k_2\frac{\partial^3\theta}{\partial x\partial y^2} + B_{66}^s\left(A' k_1 + B' k_2\right)\frac{\partial^3\theta}{\partial x\partial y} \\ &+L\frac{\partial\varphi_z}{\partial x} = I_0\ddot{u}_0 - I_1\frac{\partial\ddot{w}_0}{\partial x} - J_1\frac{\partial\ddot{\theta}}{\partial x} \end{aligned} \tag{21a}$$

$$A_{12}\frac{\partial^2 u_0^1}{\partial x\partial y}+A_{22}\frac{\partial^2 v_0^1}{\partial y^2}+A_{66}\left(\frac{\partial^2 u_0^1}{\partial x\partial y}+\frac{\partial^2 v_0^1}{\partial x^2}\right)-B_{12}\frac{\partial^3 w_0^1}{\partial x^2\partial y}$$
$$-B_{22}\frac{\partial^3 w_0^1}{\partial y^3}-2B_{66}\frac{\partial^3 w_0^1}{\partial x^2\partial y}+B_{12}^s A'k_1\frac{\partial^3\theta^1}{\partial x^2\partial y}$$
$$B_{22}^s B'k_2\frac{\partial^3\theta^1}{\partial y^3}+B_{66}^s\left(A'k_1+B'k_2\right)\frac{\partial^3\theta^1}{\partial x^2\partial y}$$
$$+L\frac{\partial\varphi_z}{\partial y}=I_0\ddot{v}_0-I_1\frac{\partial\ddot{w}_0}{\partial y}-J_1\frac{\partial\ddot{\theta}}{\partial y} \quad (21b)$$

$$B_{11}\frac{\partial^3 u_0}{\partial x^3}+B_{12}\left(\frac{\partial^3 u_0}{\partial x\partial y^2}+\frac{\partial^3 v_0}{\partial x^2\partial y}\right)+B_{22}\frac{\partial^3 v_0}{\partial y^3}$$
$$+2B_{66}\left(\frac{\partial^3 u_0}{\partial x\partial y^2}+\frac{\partial^3 v_0}{\partial x^2\partial y}\right)-D_{11}\frac{\partial^4 w_0}{\partial x^4}-2D_{12}\frac{\partial^4 w_0}{\partial x^2\partial y^2}$$
$$-D_{22}\frac{\partial^4 w_0}{\partial y^4}-4D_{66}\frac{\partial^4 w_0}{\partial x^2\partial y^2}+D_{11}^s A'k_1\frac{\partial^4\theta}{\partial x^4}$$
$$+D_{12}^s\left(A'k_1+B'k_2\right)\frac{\partial^4\theta}{\partial x^2\partial y^2}+D_{22}^s B'k_2\frac{\partial^4\theta}{\partial y^4} \quad (21c)$$
$$+2D_{66}^s\left(A'k_1+B'k_2\right)\frac{\partial^4\theta}{\partial x^2\partial y^2}+L^a\left(\frac{\partial^2\varphi_z}{\partial x^2}+\frac{\partial^2\varphi_z}{\partial y^2}\right)+q=$$
$$I_0\left(\ddot{w}_0+\ddot{\theta}\right)+J_1\left(\frac{\partial\ddot{u}_0}{\partial x}+\frac{\partial\ddot{v}_0}{\partial y}\right)-J_2\frac{\partial^4\ddot{w}_0}{\partial x^2\partial y^2}-K_2\frac{\partial^4\ddot{\theta}}{\partial x^2\partial y^2}+J_1^s\ddot{\varphi}$$

$$-B_{11}^s A'k_1\frac{\partial^3 u_0}{\partial x^3}-B_{12}^s\left(A'k_1\frac{\partial^3 v_0}{\partial x^2\partial y}+B'k_2\frac{\partial^3 u_0}{\partial x\partial y^2}\right)-B_{22}^s B'k_2\frac{\partial^3 v_0}{\partial y^3}$$
$$-B_{66}^s\left(\left(A'k_1+B'k_2\right)\frac{\partial^3 u_0}{\partial x\partial y^2}+\left(A'k_1+B'k_2\right)\frac{\partial^3 v_0}{\partial x^2\partial y}\right)+D_{11}^s A'k_1\frac{\partial^4 w_0}{\partial x^4}+D_{12}^s\left(A'k_1+B'k_2\right)\frac{\partial^4 w_0}{\partial x^2\partial y^2}$$
$$+D_{22}^s B'k_2\frac{\partial^4 w_0}{\partial y^4}+2D_{66}^s\left(A'k_1+B'k_2\right)\frac{\partial^4 w_0}{\partial x^2\partial y^2}-H_{11}^s\left(A'k_1\right)^2\frac{\partial^4\theta}{\partial x^4}-2H_{12}^s A'k_1B'k_2\frac{\partial^4\theta}{\partial x^2\partial y^2} \quad (21d)$$
$$-H_{22}^s\left(B'k_2\right)^2\frac{\partial^4\theta^1}{\partial y^4}-H_{66}^s\left(A'k_1+B'k_2\right)^2\frac{\partial^4\theta}{\partial x^2\partial y^2}+A_{44}^s\left(A'k_1\right)^2\frac{\partial^2\theta^1}{\partial x^2}+A_{55}^s\left(B'k_2\right)^2\frac{\partial^2\theta}{\partial y^2}+R\left(\frac{\partial^2\varphi_z}{\partial x^2}+\frac{\partial^2\varphi_z}{\partial y^2}\right)$$
$$+A_{44}^s\frac{\partial^2\varphi_z}{\partial x^2}+A_{55}^s\frac{\partial^2\varphi_z}{\partial y^2}+q=I_0\left(\ddot{w}_0+\ddot{\theta}\right)+J_1\left(\frac{\partial\ddot{u}_0}{\partial x}+\frac{\partial\ddot{v}_0}{\partial y}\right)-J_2\frac{\partial^4\ddot{w}_0}{\partial x^2\partial y^2}-K_2\frac{\partial^4\ddot{\theta}}{\partial x^2\partial y^2}+J_1^s\ddot{\varphi}$$

$$L\left(\frac{\partial u_0}{\partial x}+\frac{\partial v_0}{\partial y}\right)-L^a\left(\frac{\partial^2 w_0}{\partial x^2}+\frac{\partial^2 w_0}{\partial y^2}\right)-\left(R+A_{44}^s\right)\frac{\partial^2\theta}{\partial x^2}$$
$$-\left(R+A_{55}^s\right)\frac{\partial^2\theta}{\partial y^2}+R^a\varphi-A_{44}^s\frac{\partial^2\varphi_z}{\partial x^2}-A_{55}^s\frac{\partial^2\varphi_z}{\partial y^2} \quad (21e)$$
$$=J_1^s\left(\ddot{w}_0+\ddot{\theta}\right)+K_2^s\ddot{\varphi}$$

5. Exact solution for simply supported FG plate

Rectangular plates are generally classified according to the type of support used. This paper is concerned with the exact solutions of Eqs. (21a)-(21e) for a simply supported FG plate.

The following boundary conditions are imposed at the edges

$$v_0=w_0=\theta=\frac{\partial\theta}{\partial y}=\varphi=N_x=M_x^b=M_x^s=0 \text{ at } x=0,a \quad (22a)$$

$$u_0=w_0=\theta=\frac{\partial\theta}{\partial x}=\varphi=N_y=M_y^b=M_y^s=0 \text{ at } y=0,b \quad (22b)$$

Table 1 Material properties of the FG plate

Properties	Metal	Ceramic	
	Al	Al_2O_3	ZrO_2
E (GPa)	70	380	211
υ	0.3	0.3	0.3
ρ (kg/m^3)	2,702	3,800	4,500

Following the Navier solution procedure, the authors assume the following solution from for $\boldsymbol{u_0}$, $\boldsymbol{v_0}$, $\boldsymbol{w_0}$, $\boldsymbol{\theta}$ and $\boldsymbol{f_z}$ that satisfies the boundary conditions given in Eq. (22)

$$\begin{Bmatrix}u_0\\v_0\\w_0\\\theta\\\varphi^z\end{Bmatrix}=\sum_{m=1}^{\infty}\sum_{n=1}^{\infty}\begin{Bmatrix}U_{mn}e^{iwt}\cos(\lambda x)\sin(\mu y)\\V_{mn}e^{iwt}\sin(\lambda x)\cos(\mu y)\\W_{mn}e^{iwt}\sin(\lambda x)\sin(\mu y)\\X_{mn}e^{iwt}\sin(\lambda x)\sin(\mu y)\\\Phi_{mn}e^{iwt}\sin(\lambda x)\sin(\mu y)\end{Bmatrix} \quad (23)$$

Where U_{mn}, V_{mn}, W_{mn}, X_{mn} and Φ_{mn} are arbitrary parameters to be determined, ω is the is the natural frequency; and λ, μ are defined as

$$\mu=m\pi/a \quad \text{And} \quad \beta=n\pi/b \quad (24)$$

The transverse load q is also expanded in the double-Fourier sine series as

$$q(x,y)=\sum_{m=1}^{\infty}\sum_{n=1}^{\infty}q_{mn}\sin(\lambda x)\sin(\mu y) \quad (25a)$$

For the case of a sinusoidally distributed load, it is

$$m=n=1 \quad \text{and} \quad q_{11}=q_0 \quad (25b)$$

Where q_0= intensity of the load at the plate center.
For the case of a uniformly distributed load (UDL), it is

$$q_{mn}=\frac{16q_0}{mn\pi^2},\quad (m,n=1,3,5,\ldots) \quad (25c)$$

Substituting Eqs. (23) and (25) into Eq. (21), the analytical solutions can be obtained from

$$\left(\begin{bmatrix}a_{11}&a_{12}&a_{13}&a_{14}&a_{15}\\a_{12}&a_{22}&a_{23}&a_{24}&a_{25}\\a_{13}&a_{23}&a_{33}&a_{34}&a_{35}\\a_{14}&a_{24}&a_{34}&a_{44}&a_{45}\\a_{15}&a_{25}&a_{35}&a_{45}&a_{55}\end{bmatrix}-\omega^2\begin{bmatrix}m_{11}&0&m_{13}&m_{14}&0\\0&m_{22}&m_{23}&m_{24}&0\\m_{13}&m_{23}&m_{33}&m_{34}&m_{35}\\m_{14}&m_{24}&m_{34}&m_{44}&m_{45}\\0&0&m_{35}&m_{45}&m_{55}\end{bmatrix}\right)\begin{Bmatrix}U_{mn}\\V_{mn}\\W_{mn}\\X_{mn}\\\Phi_{mn}\end{Bmatrix}=\begin{Bmatrix}0\\0\\q_{mn}\\q_{mn}\\0\end{Bmatrix} \quad (26)$$

In which

Table 2 Effect of normal strain ε_z on dimensionless stresses and transversal displacement for isotropic square plate subjected to uniformly distributed load (U.D.L) (a/h=10)

Theory	$\hat{w}(a/2,b/2,0)$	$\hat{\sigma}_x(h/2)$	$\hat{\sigma}_y(h/2)$	$\hat{\tau}_{xy}(h/2)$	$\hat{\tau}_{xz}(0,b/2,0)$	$\hat{\tau}_{yz}(a/2,0,0)$
Present $\varepsilon_Z\neq0$	4.628	0.268	0.268	0.194	0.491	0.491
Hebali *et al.* (2014) $\varepsilon_Z\neq0$	4.631	0.276	0.276	0.197	0.481	0.481
Shimpi *et al.* (2003) $\varepsilon_Z\neq0$	4.625	0.307	0.307	0.195	0.505	0.505
Exact 3D (Srinivas *et al.* 1970a)	4.639	0.290	0.290	—	488	—

Table 3 Effects of volume fraction exponent on the dimensionless stresses and deflections of a FG square plate subjected to Sinusoidal Load

	$\bar{w}(0)$		$\hat{\sigma}_x(1/2)$		$\hat{\sigma}_y(1/3)$	
	Present	Hebali *et al.* (2014)	Present	Hebali *et al.* (2014)	Present	Hebali *et al.* (2014)
k	$\varepsilon_z\neq0$	$\varepsilon_z\neq0$	$\varepsilon_z\neq0$	$\varepsilon_z\neq0$	$\varepsilon_z\neq0$	$\varepsilon_z\neq0$
Ceramic	0.2936	0.2937	1.8599	1.9076	1.3604	1.3451
1	0.5685	0.5689	2.8296	2.9105	1.5176	1.4954
2	0.7220	0.7220	3.3322	3.4198	1.4195	1.3953
3	0.7980	0.7972	3.5830	3.6729	1.2975	1.2729
4	0.8421	0.8413	3.7654	3.8569	1.2021	1.1779
5	0.8732	0.8729	3.9354	4.0273	1.1285	1.1049
6	0.8991	0.8983	4.1024	4.1954	1.0692	1.0462
7	0.9215	0.9211	4.2671	4.3619	1.0192	0.9976
8	0.9424	0.9416	4.4293	4.5251	0.9763	0.9546
9	0.9614	0.9606	4.5876	4.6846	0.9396	0.9203
10	0.9796	0.9793	4.7396	4.8388	0.9077	0.8908
Metal	1.5936	1.5942	1.8599	1.9076	1.3604	1.3451

$$
\begin{aligned}
a_{11} &= -(A_{11}\alpha^2 + A_{66}\beta^2)\\
a_{12} &= -\alpha\,\beta\,\left(A_{12} + A_{66}\right)\\
a_{13} &= \alpha(B_{11}\alpha^2 + (B_{12} + 2B_{66})\beta^2)\\
a_{14} &= -\alpha(B_{11}^s A'k_1\alpha^2 + B_{12}^s B'k_2\beta^2 + B_{66}^s\left(A'k_1 + B'k_2\right)\beta^2)\\
a_{15} &= L\alpha\\
a_{22} &= -\alpha^2 A_{66} - \beta^2 A_{22}\\
a_{22} &= -\alpha^2 A_{66} - \beta^2 A_{22}\\
a_{23} &= \beta(B_{22}\beta^2 + (B_{12} + 2B_{66})\alpha^2)\\
a_{24} &= -\beta\left(B_{22}^s B'k_2\beta^2 + \alpha^2\left(B_{12}^s A'k_1 + B_{66}^s\left(A'k_1 + B'k_2\right)\right)\right)\\
a_{25} &= L\beta\\
a_{33} &= -\alpha^2\left(D_{11}\alpha^2 + \left(2D_{12} + 4D_{66}\right)\beta^2\right) - D_{22}\beta^4\\
a_{34} &= D_{11}^s A'k_1\alpha^4 + D_{12}^s\left(A'k_1 + B'k_2\right)\beta^2\alpha^2\\
&\quad + D_{22}^s B'k_2\beta^4 + 2D_{66}^s\left(A'k_1 + B'k_2\right)\beta^2\alpha^2\\
a_{35} &= -L^a(\alpha^2 + \beta^2)\\
a_{44} &= -(H_{11}^s\alpha^2 k_1 + 2k_1\beta^2 H_{66}^s + 2H_{66}^s\alpha^2 k_2 + H_{12}^s\alpha^2 k_2\\
&\quad + k_1\beta^2 H_{12}^s + k_2\beta^2 H_{22}^s + A_s^{44}k_1 + A_s^{55}k_2)\\
a_{45} &= -[A_{44}^s\alpha^2 + A_{55}^s\beta^2 + R(\alpha^2 + \beta^2)]\\
a_{55} &= -(A_{44}^s\alpha^2 + A_{55}^s\beta^2 + R^a)
\end{aligned}
\tag{27}
$$

And

$$
\begin{aligned}
m_{11} &= m_{22} = -I_0\\
m_{13} &= \alpha I_1\\
m_{14} &= \alpha J_1\\
m_{23} &= \beta I_1\\
m_{24} &= \beta J_1\\
m_{33} &= -[I_0 + I_2(\alpha^2 + \beta^2)]\\
m_{34} &= -[I_0 + J_2(\alpha^2 + \beta^2)]\\
m_{44} &= -[I_0 + K_2(\alpha^2 + \beta^2)]\\
m_{35} &= m_{45} = -J_1^s\\
m_{55} &= -K_2^s
\end{aligned}
\tag{28}
$$

6. Numerical results

In this section, various numerical examples are presented for bending and free vibration analyses of a simply supported FG plate.

The proposed model for bending and free vibration of FG plate will be first validated through the comparison with the existing data available in literature. For this, two types of FGMs plates are considered: Al/Al_2O_3 and Al/ZrO_2.

Table 3 Effect of normal strain σ_z on dimensionless in-plane longitudinal $\bar{\sigma}_x$ stresses and displacement $\bar{w}$ for FG square plate subjected to Sinusoidal Load

		$\bar{\sigma}_x(h/3)$			$\bar{w}(a/2,b/2,0)$		
k	Theory	a/h=4	a/h=10	a/h=100	a/h=4	a/h=10	a/h=100
1	Present $\varepsilon_z \neq 0$	0,6018	1,5180	15,200	0,6965	0,5685	0,5438
	Carrera *et al.* (2011) $\varepsilon_z = 0$	0.7856	2.0068	20.149	0.7289	0.5890	0.5625
	Carrera *et al.* (2011) $\varepsilon_z \neq 0$	0.6221	1.5064	14.969	0.7171	0.5875	0.5625
	Neves *et al.* (2012) $\varepsilon_z \neq 0$	0.5925	1.4945	14.969	0.6997	0.5845	0.5624
	Hebali *et al.* (2014) $\varepsilon_z \neq 0$	0.5952	1.4954	14.963	0.6910	0.5686	0.5452
4	Present $\varepsilon_z \neq 0$	0,4581	1,2020	12,120	1,1080	0,8421	0,7912
	Carrera *et al.* (2011) $\varepsilon_z = 0$	0.5986	1.5874	16.047	1.1673	0.8828	0.8286
	Carrera *et al.* (2011) $\varepsilon_z \neq 0$	0.4877	1.1971	11.923	1.1585	0.8821	0.8286
	Neves *et al.* (2012) $\varepsilon_z \neq 0$	0.4404	1.1783	11.932	1.1178	0.8750	0.8286
	Hebali *et al.* (2014) $\varepsilon_z \neq 0$	0.4507	1.1779	11.871	1.0964	0.8413	0.7926
10	Present $\varepsilon_z \neq 0$	0,3380	1,9077	9,2060	1,3500	0,9796	0,9090
	Carrera *et al.* (2011) $\varepsilon_z = 0$	0.4345	1.1807	11.989	1.3925	1.0090	0.9361
	Carrera *et al.* (2011) $\varepsilon_z \neq 0$	0.1478	0.8965	8.9077	1.3745	1.0072	0.9361
	Neves *et al.* (2012) $\varepsilon_z \neq 0$	0.3227	1.1783	11.932	1.3490	0.8750	0.8286
	Hebali *et al.* (2014) $\varepsilon_z \neq 0$	0.3325	0.8889	8.9977	1.3333	0.9791	0.9114

The material properties of FG plates are reported in Table 1.

For convenience, the following dimensionless forms are used

$$\bar{z}=\frac{z}{h},\quad S=\frac{a}{h},\quad \bar{w}=\frac{10E_c}{q_0 a S^3}w(\frac{a}{2},\frac{b}{2},\bar{z}),\quad \hat{w}=\frac{100E}{q_0 h S^4}w(\frac{a}{2},\frac{b}{2},\bar{z}),$$

$$\bar{\sigma}_x=\frac{1}{q_0 S}\sigma_x(\frac{a}{2},\frac{b}{2},\bar{z}),\quad \hat{\sigma}_x=\frac{1}{q_0 S^2}\sigma_x(\frac{a}{2},\frac{b}{2},\bar{z})$$

$$\bar{\sigma}_y=\frac{1}{q_0 S}\sigma_y(\frac{a}{2},\frac{b}{2},\bar{z}),\quad \hat{\sigma}_y=\frac{1}{q_0 S^2}\sigma_y(\frac{a}{2},\frac{b}{2},\bar{z})$$

$$\bar{\tau}_{xy}=\frac{1}{q_0 S}\tau_{xy}(0,0,\bar{z}),\quad \hat{\tau}_{xy}=\frac{1}{q_0 S^2}\tau_{xy}(0,0,\bar{z})$$

$$\bar{\tau}_{yz}=\frac{1}{q_0 S}\tau_{yz}(\frac{a}{2},0,\bar{z}),\quad \bar{\tau}_{xz}=\frac{1}{q_0 S}\tau_{xz}(0,\frac{b}{2},\bar{z})$$

$$\bar{\omega}=\omega\frac{a^2}{h}\sqrt{\rho_c/E_c},\hat{\omega}=\omega h\sqrt{\rho/E}$$

6.1 Bending analysis

The Young's modulus and Poisson's ratio used for this example are 210 GPa and 0,3 respectively.

In order to prove the validity of the present improved higher shear deformation theory, comparisons are made between the results obtained from this theory and those obtained by Hebali *et al.* (2014), Shimpi *et al.* (2003), exact solution developed by Srinivas *et al.* (1970a), quasi-3D theory given by Neves *et al.* (2012) and finite-element approximations presented by Carrera *et al.* (2011).

As a first example, an isotropic plate subjected to a uniformly distributed load is studied.

Displacement results and stress are compared with the quasi-three-dimensional (3D) hyperbolic shear deformation theory given by Hebali *et al.* (2014), solutions given by Shimpi *et al.* (2003), and the exact solution presented by

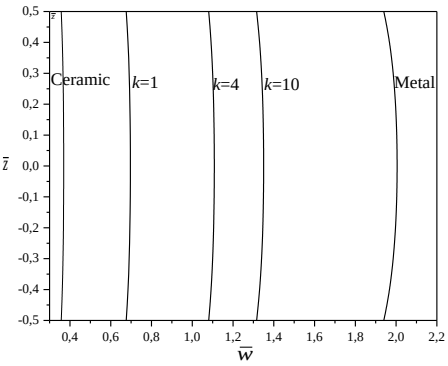

Fig. 1 The transverse displacement $\bar{w}$ through the thickness of FG plate (*a/h*=4) subjected to sinusoidal load

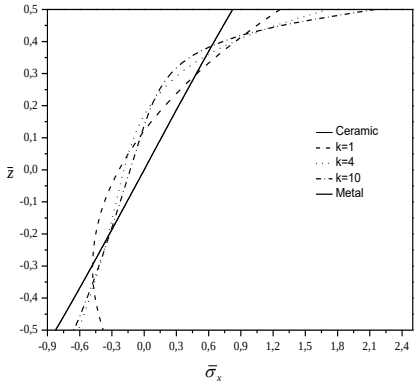

Fig. 2 Variation of axial stress $\bar{\sigma}_x$ through-the-thickness of square FG plate (*a/h*=4) subjected to sinusoidal load

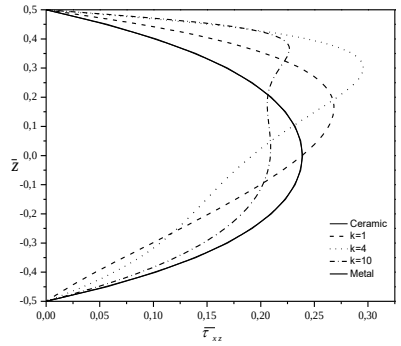

Fig. 3 Variation of transverse shear stress $\bar{\tau}_{xz}$ through-the-thickness of square FG plate (*a/h=4*) subjected to sinusoidal load

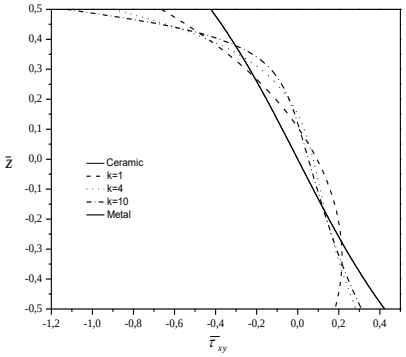

Fig. 4 Variation of in-plane tangential stress $\bar{\tau}_{xy}$ through-the-thickness of square FG plate (*a/h*=4) subjected to sinusoidal load

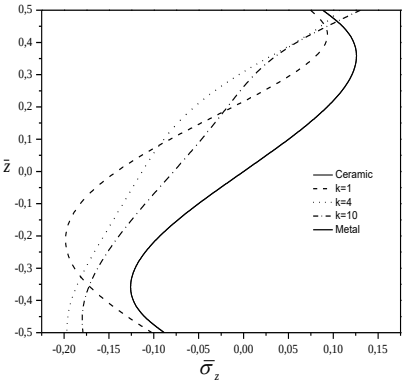

Fig. 5 Variation of transverse normal stress $\bar{\sigma}_z$ through-the-thickness of square FG plate (*a/h*=4) subjected to sinusoidal load

Srinivas *et al.* (1970a).

It can be observed from the results listed in Table 2 that our results are in a good agreement with the others.

The second example studied is that of a thick AL/AL_2O_3 plate subjected to a sinusoidal load.

The results of the stresses and displacement are given for three values of the power index *k* as shown in Table 3.

According to the results presented in this table, it can be seen that the results of the present improved method are in very great agreement with those of the solutions taking into account the stretching effect ($\varepsilon_z \neq 0$) namely those of Carrera *et al.* (2011) and Hebali *et al.* (2014) and whether it is for displacement or stress. Also, an existing difference between the results of this method and those of Carrera *et al.* (2011) for the case where the stretching effect is neglected ($\varepsilon_z=0$) is noted. This can be explained by the fact that the stretching effect has great influence in the results of thick plates.

Table 4 Natural frequencies $\hat{\omega} = \omega h\sqrt{\rho/E}$ of an Isotropic Plate with υ=0.3, *a/h*=10 and *a/b*=1

m	n	Present	Hebali *et al.* (2014) $\varepsilon_z \neq 0$	Srinivas *et al.* (1970b) (3D)	Reddy and Phan (1985)	Whitney and Pagano (1970)
1	1	0.0930	0.0933	0.0932	0.0931	0.0930
1	2	0.2229	0.2228	0.2226	0.2222	0.2220
2	2	0.3425	0.3422	0.3421	0.3411	0.3406
1	3	0.4176	0.4173	0.4171	0.4158	0.4149
2	3	0.5243	0.5240	0.5239	0.5221	0.5206
3	3	0.6893	0.6890	0.6889	0.6862	0.6834
2	4	0.7513	0.7512	0.7511	0.7481	0.7447
1	5	0.9270	0.9268	0.9268	0.9230	0.9174
4	4	1.0891	1.0890	1.0889	1.0847	1.0764

The displacement and the calculated stresses are those of a rectangular FG plate subjected to a sinusoidal load.

Again, the results of this improved method are very consistent with those of Hebali *et al.* (2014).

After this series of results comparison, it can be said that the present method is accurate for the analysis of the bending of FG plates.

The influence of the volume fraction index *k* on the variation of the transverse displacement $\bar{w}$ through the thickness direction is showed in Fig. 1 for a FG plate subjected to sinusoidal load. It can be seen from this figure that the displacement of metal plates is larger than the corresponding one of ceramic plates and that the displacement increases as the power law index *k* increases.

Fig. 2 plots the variation of axial stress $\bar{\sigma}_x$ through the thickness of square FG plate (*a/h*=4) subjected to sinusoidal load. It can be observed that the axial stress $\bar{\sigma}_x$ is tensile at the top surface and compressive at the bottom surface and the homogeneous ceramic or metal plate gives the maximum stresses at the bottom surface and the minimum tensile stresses at the top surface of the plate.

In Fig. 3, we present the variation of transverse shear stress $\bar{\tau}_{xz}$ through the thickness of square FG plate (a/h=4) subjected to sinusoidal load.

As can be seen in Fig. 3, the distribution of the transverse shear stresses $\bar{\tau}_{xz}$ is parabolic for the cases of homogeneous ceramic or metal and this is not the case for other types of plates.

Fig. 4 depicts the variation of the stress $\bar{\tau}_{xy}$ through the thickness of square FG plate subjected to sinusoidal load. The same observation establishes for the case of axial stress $\bar{\sigma}_x$ remains valid for this case namely, the stresses $\bar{\tau}_{xy}$ are

Table 5a Natural frequencies of rectangular FG (a/h=10 and a/b=0.5)

	k=0				k=0.5			
Mode(m,n)	Present	Hebali *et al.* (2014)	Jha *et al.* (2012)	Shahrjerdi *et al.* (2011)	Present	Hebali *et al.* (2014)	Jha *et al.* (2012)	Shahrjerdi *et al.* (2011)
1(1,1)	3.6628	3.6959	3.6911	3.6983	3.3584	3.3877	3.3664	3.3713
2(1,2)	5.7889	5.8392	5.8323	5.8498	5.3118	5.3564	5.3238	5.3359
3(2,1)	11.8820	11.9752	11.965	12.0345	10.9247	11.0079	10.946	10.9940
4(2,2)	13.8275	13.9324	13.921	14.0144	12.7212	12.8149	12.745	12.8103
5(2,3)	16.9850	17.1070	17.096	17.2325	15.6408	15.7500	15.668	15.7660
6(3,2)	25.8985	26.0579	26.051	26.3462	23.9071	24.0503	23.941	24.1494
7(3,3)	28.7071	28.8754	28.871	29.2257	26.5186	26.6697	26.554	26.8100

Table 5b Natural frequencies of rectangular FG (a/h=10 and a/b=0.5)

	k=1				k=2			
Mode(m,n)	Present	Hebali *et al.* (2014)	Jha *et al.* (2012)	Shahrjerdi *et al.* (2011)	Present	Hebali *et al.* (2014)	Jha *et al.* (2012)	Shahrjerdi *et al.* (2011)
1(1,1)	3.2262	3.2550	3.1291	3.1354	3.1484	3.1757	3.1291	3.1354
2(1,2)	5.1021	5.1460	4.9434	4.9594	4.9747	5.0157	4.9434	4.9594
3(2,1)	10.4907	10.5720	10.137	10.1985	10.2037	10.2776	10.137	10.1985
4(2,2)	12.2147	12.3062	11.794	11.8784	11.8721	11.9543	11.794	11.8784
5(2,3)	15.0162	15.1225	14.481	14.6092	14.5786	14.6726	14.481	14.6092
6(3,2)	22.9453	23.0833	22.059	22.3273	22.2125	22.3285	22.059	22.3273
7(3,3)	25.4494	25.5947	24.446	24.7781	24.6163	24.7361	24.446	24.7781

tensile at the top surface and compressive at the bottom surface and the isotropic ceramic or metal plate gives the maximum stresses at the bottom surface and the minimum tensile stresses at the top surface of the plate.

In Fig. 5, we have plotted the through the thickness distributions of the transverse shear stresses $\overline{\sigma}_z$.

It can be concluded from this figure that the transverse normal component $\overline{\sigma}_z$ cannot be neglected for the present problem.

6.2 Free vibration analysis

Other examples to verify the accuracy of the present theory in predicting the natural frequency of FG AL/ZrO_2 plates are reported in Tables 4 and 5.

Table 4 gives a comparison of the natural frequencies $\hat{\omega}$ of square rectangular think plates (a/h = 10) between the present results and those of the quasi-three-dimensional (3D) hyperbolic shear deformation theory given by Hebali *et al.* (2014), the three-dimensional (3D) elasticity solutions developed by Srinivas *et al.* (1970b), the higher-order shear deformation theory presented by Reddy and Phan (1985), and with the first shear deformation theory of Whitney and Pagano (1970).

An excellent agreement between the different results is obtained, particularly between the present theory and 3D hyperbolic shear deformation theory and the 3D elasticity solutions.

It should be noted that the slight difference that exists between the present solution and the two other amounts to the fact that the latter neglect the stretching effect.

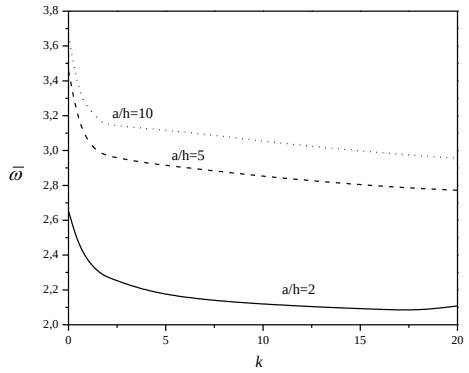

Fig. 6 Variation of the Non-dimensional fundamental natural frequency $\overline{\omega}$ of simply supported FG plate rectangular plates (b=2a) versus the power law index k

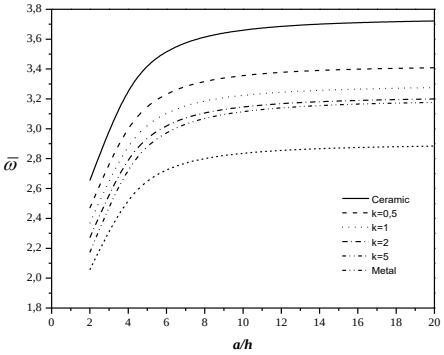

Fig. 7 Variation of the Non-dimensional fundamental natural frequency $\overline{\omega}$ of simply supported FG plate rectangular plates (b=2a) versus the side-to-thickness ratio (a/h)

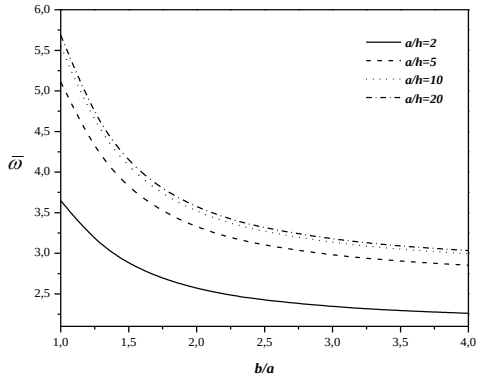

Fig. 8 Variation of the Non-dimensional fundamental natural frequency $\bar{\omega}$ of simply supported FG plate versus the aspect ratio b/a (k=0.2)

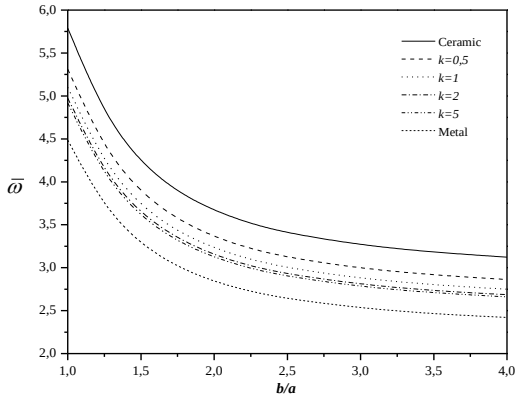

Fig. 8 V Variation of the Non-dimensional fundamental natural frequency $\bar{\omega}$ of simply supported FG versus the aspect ratio b/a (a/h=10)

In Table 5 (a and b), we present a comparison of the nondimensional frequencies $\bar{\omega}$ of a think AL/ZrO_2 FG plates predicted by the present theory and the solution presented by Hebali *et al.* (2014), the higher-order shear and normal deformation theory given by Jha *et al.* (2012) and the second-order shear deformation theory developed by Shahrjerdi *et al.* (2011).

Once again, a good agreement between the results is obtained for all vibration modes which confirm the accuracy of the present theory.

The Fig. 6 illustrates the variation of the non-dimensional fundamental natural frequency $\bar{\omega}$ of simply supported FG plate rectangular plates versus the power law index k and for three values of the side-to-thickness ratios a/h. It has seen a rapid increase of the non-dimensional fundamental natural frequency until a value of k = 2, Once exceeding this value, the natural frequency tends to keep a more or less constant shape. On the other hand, the increase in the A/h ratio tends to decrease frequencies. In other words, the thicker the plate becomes, the lower the frequencies.

The Fig. 6 illustrates the variation of the non-dimensional fundamental natural frequency $\bar{\omega}$ of simply supported FG plate rectangular plates versus the power law index k and for three values of the side-to-thickness ratios a/h. It has seen a rapid increase of the non-dimensional fundamental natural frequency until a value of k = 2, Once exceeding this value, the natural frequency tends to keep a more or less constant shape. On the other hand, the increase in the A/h ratio tends to decrease frequencies. In other words, the thicker the plate becomes, the lower the frequencies.

Fig. 7 plots the variation of the non-dimensional fundamental natural frequency $\bar{\omega}$ of simply supported FG plate rectangular plates as a function the side-to-thickness ratio (a/h). As can be seen, the increase in the a/h ratio increases the frequency and the increase in the power index k reduces them. Also, the homogeneous ceramic plate has the highest frequency.

In Fig. 8 we present the variation of the non-dimensional fundamental natural frequency $\bar{\omega}$ of simply supported FG plate versus the aspect ratio b/a and for different values of the side-to-thickness ratios a/h. The highest frequencies are obtained for a square plate (b/a = 1). The more rectangular the plate becomes, the frequencies relapse.

In Fig. 9, we have plotted the same variation but for different values of the power law index k.

The highest frequencies are obtained for a homogeneous ceramic plate and the lowest for a metal plate. The increase in index k decreases the frequencies.

7. Conclusions

In this study, bending and free vibration analysis of functionally graded plate is carried out by an improved higher shear deformation theory taking into account the influence of stretching effect.

The kinematic of the present improved theory is modified by considering undetermined integral terms in in-plane displacements which results in a reduced number of variables compared with other shear deformation theory of the same order. Navier solution was used to find the different parameters governing the bending and free vibration of these plates. Verification examples demonstrate that the developed theory is not only more accurate than the refined plate theory, but also comparable with the HSDTs which use more number of variables.

References

Abdelaziz, H.H., Ait Amar Meziane, M., Bousahla, A.A., Tounsi, A., Mahmoud, S.R. and Alwabli, A.S. (2017), "An efficient hyperbolic shear deformation theory for bending, buckling and free vibration of FGM sandwich plates with various boundary conditions", *Steel Compos. Struct.*, **25**(6), 693-704.

Abualnour, M., Houari, M.S.A., Tounsi, A., Adda Bedia, E.A. and Mahmoud, S.R. (2018), "A novel quasi-3D trigonometric plate theory for free vibration analysis of advanced composite plates", *Compos. Struct.*, **184**, 688-697.

Ahmed, A. (2014), "Post buckling analysis of sandwich beams with functionally graded faces using a consistent higher order theory", *J. Civil Struct. Environ.*, **4**(2), 59-64.

Ahouel, M., Houari, M.S.A., Adda Bedia, E.A. and Tounsi, A. (2016), "Size-dependent mechanical behavior of functionally graded trigonometric shear deformable nanobeams including neutral surface position concept", *Steel Compos. Struct.*, **20**(5), 963-981.

Huffington, N.J. (1963), "Response of elastic columns to axial pulse loading", *AIAA J.*, **1**(9), 2099-2104.

Ait Amar Meziane, M., Abdelaziz, H.H. and Tounsi, A. (2014), "An efficient and simple refined theory for buckling and free vibration of exponentially graded sandwich plates under various boundary conditions", *J. Sandw. Struct. Mater.*, **16**(3), 293-318.

Ait Yahia, S., Ait Atmane, H., Houari, M.S.A. and Tounsi, A. (2015), "Wave propagation in functionally graded plates with porosities using various higher-order shear deformation plate theories", *Struct. Eng. Mech.*, **53**(6), 1143-1165.

Akavci, S.S. (2016), "Mechanical behavior of functionally graded sandwich plates on elastic foundation", *Compos. Part B*, **96**, 136-152.

Al-Basyouni, K.S., Tounsi, A. and Mahmoud, S.R. (2015), "Size dependent bending and vibration analysis of functionally graded micro beams based on modified couple stress theory and neutral surface position", *Compos. Struct.*, **125**, 621-630.

Arani, A.J. and Kolahchi, R. (2016), "Buckling analysis of embedded concrete columns armed with carbon nanotubes", *Comput. Concrete*, **17**(5), 567-578.

Attia, A., Tounsi, A., Adda Bedia, E.A. and Mahmoud, S.R. (2015), "Free vibration analysis of functionally graded plates with temperature-dependent properties using various four variable refined plate theories", *Steel Compos. Struct.*, **18**(1), 187-212.

Attia, A., Bousahla, A.A., Tounsi, A., Mahmoud, S.R. and Alwabli, A.S. (2018), "A refined four variable plate theory for thermoelastic analysis of FGM plates resting on variable elastic foundations", *Struct. Eng. Mech.*, In Press.

Bakhadda, B., Bachir Bouiadjra, M., Bourada, F., Bousahla, A.A., Tounsi, A. and Mahmoud, S.R. (2018), "Dynamic and bending analysis of carbon nanotube-reinforced composite plates with elastic foundation", *Wind Struct.*, Accepted.

Barati, M.R. and Shahverdi, H. (2016), "A four-variable plate theory for thermal vibration of embedded FG nanoplates under non-uniform temperature distributions with different boundary conditions", *Struct. Eng. Mech.*, **60**(4), 707-727.

Baseri, V., Jafari, G.R.S. and Kolahchi, R. (2016), "Analytical solution for buckling of embedded laminated plates based on higher order shear deformation plate theory", *Steel Compos. Struct.*, **21**(4), 883-919.

Belabed, Z., Houari, M.S.A., Tounsi, A., Mahmoud, S.R. and Anwar Bég, O. (2014), "An efficient and simple higher order shear and normal deformation theory for functionally graded material (FGM) plates", *Compos. Part B*, **60**, 274-283.

Beldjelili, Y., Tounsi, A. and Mahmoud, S.R. (2016), "Hygro-thermo-mechanical bending of S-FGM plates resting on variable elastic foundations using a four-variable trigonometric plate theory", *Smart Struct. Syst.*, **18**(4), 755-786.

Belkorissat, I., Houari, M.S.A., Tounsi, A., Adda Bedia, E.A. and Mahmoud, S.R. (2015), "On vibration properties of functionally graded nano-plate using a new nonlocal refined four variable model", *Steel Compos. Struct.*, **18**(4), 1063-1081.

Bellifa, H., Benrahou, K.H., Hadji, L., Houari, M.S.A. and Tounsi, A. (2016), "Bending and free vibration analysis of functionally graded plates using a simple shear deformation theory and the concept the neutral surface position", *J. Braz. Soc. Mech. Sci. Eng.*, **38**, 265-275.

Bellifa, H., Benrahou, K.H., Bousahla, A.A., Tounsi, A. and Mahmoud, S.R. (2017a), "A nonlocal zeroth-order shear deformation theory for nonlinear postbuckling of nanobeams", *Struct. Eng. Mech.*, **62**(6), 695-702.

Bellifa, H., Bakora, A., Tounsi, A., Bousahla, A.A. and Mahmoud, S.R. (2017b), "An efficient and simple four variable refined plate theory for buckling analysis of functionally graded plates", *Steel Compos. Struct.*, **25**(3), 257-270.

Benadouda, M., Ait Atmane, H., Tounsi, A., Bernard, F., Mahmoud, S.R. (2017), "An efficient shear deformation theory for wave propagation in functionally graded material beams with porosities", *Earthq. Struct.*, **13**(3), 255-265.

Benchohra, M., Driz, H., Bakora, A., Tounsi, A., Adda Bedia, E.A. and Mahmoud, S.R. (2018), "A new quasi-3D sinusoidal shear deformation theory for functionally graded plates", *Struct. Eng. Mech.*, **65**(1), 19-31.

Bennoun, M., Houari, M.S.A. and Tounsi, A. (2016), "A novel five variable refined plate theory for vibration analysis of functionally graded sandwich plates", *Mech. Adv. Mater. Struct.*, **23**(4), 423-431.

Bessaim, A., Houari, M.S.A., Tounsi, A., Mahmoud, S.R. and Adda Bedia, E.A. (2013), "A new higher order shear and normal deformation theory for the static and free vibration analysis of sandwich plates with functionally graded isotropic face sheets", *J. Sandw. Struct. Mater.*, **15**, 671-703.

Besseghier, A., Houari, M.S.A., Tounsi, A. and Mahmoud, S.R. (2017), "Free vibration analysis of embedded nanosize FG plates using a new nonlocal trigonometric shear deformation theory", *Smart Struct. Syst.*, **19**(6), 601-614.

Bilouei, B.S., Kolahchi, R. and Bidgoli, M.R. (2016), "Buckling of concrete columns retrofitted with nano-fiber reinforced polymer (NFRP)", *Comput. Concrete*, **18**(5), 1053-1063.

Bouafia, K., Kaci, A., Houari, M.S.A., Benzair, A. and Tounsi, A. (2017), "A nonlocal quasi-3D theory for bending and free flexural vibration behaviors of functionally graded nanobeams", *Smart Struct. Syst.*, **19**(2), 115-126.

Bouderba, B., Houari, M.S.A. and Tounsi, A. (2013), "Thermomechanical bending response of FGM thick plates resting on winkler-pasternak elastic foundations", Steel *Compos. Struct.*, **14**(1), 85-104.

Bouderba, B., Houari, M.S.A., Tounsi, A. and Mahmoud, S.R. (2016), "Thermal stability of functionally graded sandwich gkplates using a simple shear deformation theory", *Struct. Eng. Mech.*, **58**(3), 397-422.

Boukhari, A., Ait Atmane, H., Tounsi, A., Adda Bedia, E.A. and Mahmoud, S.R. (2016), "An efficient shear deformation theory for wave propagation of functionally graded material plates", *Struct. Eng. Mech.*, **57**(5), 837-859.

Bounouara, F., Benrahou, K.H., Belkorissat, I. and Tounsi, A. (2016), "A nonlocal zeroth-order shear deformation theory for free vibration of functionally graded nanoscale plates resting on elastic foundation", *Steel Compos. Struct.*, **20**(2), 227-249.

Bourada, M., Kaci, A., Houari, M.S.A. and Tounsi, A. (2015), "A new simple shear and normal deformations theory for functionally graded beams", *Steel Compos. Struct.*, **18**(2), 409-423.

Bousahla, A.A., Houari, M.S.A., Tounsi, A. and Adda Bedia, E.A. (2014), "A novel higher order shear and normal deformation theory based on neutral surface position for bending analysis of

advanced composite plates", *Comput. Meth.*, **11**(6), 1350082.
Bousahla, A.A., Benyoucef, S., Tounsi, A. and Mahmoud, S.R. (2016), "On thermal stability of plates with functionally graded coefficient of thermal expansion", *Struct. Eng. Mech.*, **60**(2), 313-335.
Carrera, E., Brischetto, S., Cinefra, M. and Soave, M. (2011), "Effects of thickness stretching in functionally graded plates and shells", *Compos. Part B Eng.*, **42**(2), 123-133.
Chikh, A., Tounsi, A., Hebali, H. and Mahmoud, S.R. (2017), "Thermal buckling analysis of cross-ply laminated plates using a simplified HSDT", *Smart Struct. Syst.*, **19**(3), 289-297.
Draiche, K., Tounsi, A. and Mahmoud, S.R. (2016), "A refined theory with stretching effect for the flexure analysis of laminated composite plates", *Geomech. Eng.*, **11**(5), 671-690.
El-Haina, F., Bakora, A., Bousahla, A.A., Tounsi, A. and Mahmoud, S.R. (2017), "A simple analytical approach for thermal buckling of thick functionally graded sandwich plates", *Struct. Eng. Mech.*, **63**(5), 585-595.
Fahsi, A., Tounsi, A., Hebali, H., Chikh, A., Adda Bedia, E.A. and Mahmoud, S.R. (2017), "A four variable refined nth-order shear deformation theory for mechanical and thermal buckling analysis of functionally graded plates", *Geomech. Eng.*, **13**(3), 385-410.
Fekrar, A., Houari, M.S.A., Tounsi, A. and Mahmoud, S.R. (2014), "A new five-unknown refined theory based on neutral surface position for bending analysis of exponential graded plates", *Meccan.*, **49**, 795-810.
Hachemi, H., Kaci, A., Houari, M.S.A., Bourada, A., Tounsi, A. and Mahmoud, S.R. (2017), "A new simple three-unknown shear deformation theory for bending analysis of FG plates resting on elastic foundations", *Steel Compos. Struct.*, **25**(6), 717-726.
Hadji, L., Hassaine Daouadji, T. and Adda Bedia, E. (2015), "A refined exponential shear deformation theory for free vibration of FGM beam with porosities", *Geomech. Eng.*, **9**(3), 361 - 372.
Hajmohammad, M.H., Zarei, M.S., Nouri, A. and Kolahchi, R. (2017), "Dynamic buckling of sensor/functionally graded-carbon nanotube-reinforced laminated plates/actuator based on sinusoidal-visco-piezoelasticity theories", *J. Sandw. Struct. Mater.*, In Press.
Hamidi, A., Houari, M.S.A., Mahmoud, S.R. and Tounsi, A. (2015), "A sinusoidal plate theory with 5-unknowns and stretching effect for thermomechanical bending of functionally graded sandwich plates", *Steel Compos. Struct.*, **18**(1), 235-253.
Hebali, H., Tounsi, A., Houari, M.S.A., Bessaim, A. and Adda Bedia, E.A. (2014), "New quasi-3D hyperbolic shear deformation theory for the static and free vibration analysis of functionally graded plates", *J. Eng. Mech.*, **140**, 374-383.
Houari, M.S.A., Tounsi, A., Bessaim, A. and Mahmoud, S.R. (2016), "A new simple three-unknown sinusoidal shear deformation theory for functionally graded plates", *Steel Compos. Struct.*, **22**(2), 257-276.
Jha, D.K., Kant, T. and Singh, R.K. (2012), "Higher order shear and normal deformation theory for natural frequency of functionally graded rectangular plates", *Nucl. Eng. Des.*, **250**, 8-13.
Khetir, H., Bachir Bouiadjra, M., Houari, M.S.A., Tounsi, A. and Mahmoud, S.R. (2017), "A new nonlocal trigonometric shear deformation theory for thermal buckling analysis of embedded nanosize FG plates", *Struct. Eng. Mech.*, **64**(4), 391-402.
Klouche, F., Darcherif, L., Sekkal, M., Tounsi, A. and Mahmoud, S.R. (2017), "An original single variable shear deformation theory for buckling analysis of thick isotropic plates", *Struct. Eng. Mech.*, **63**(4), 439-446.
Kolahchi, R. and Bidgoli, A.M. (2016), "Size-dependent sinusoidal beam model for dynamic instability of single-walled carbon nanotubes", *Appl. Math. Mech.*, **37**(2), 265-274.
Larbi Chaht, F., Kaci, A., Houari, M.S.A., Tounsi, A., Anwar Bég, O. and Mahmoud, S.R. (2015), "Bending and buckling analyses of functionally graded material (FGM) size-dependent nanoscale beams including the thickness stretching effect", *Steel Compos. Struct.*, **18**(2), 425-442.
Mahapatra, T.R., Kar, V.R. and Panda, V.R. (2016), "Large amplitude bending behaviour of laminated composite curved panels", *Eng. Comput. Int. J. Comput.-Aid. Eng. Softw.*, **33**(1), 116-138.
Mahi, A., Adda Bedia, E.A. and Tounsi, A. (2015), "A new hyperbolic shear deformation theory for bending and free vibration analysis of isotropic, functionally graded, sandwich and laminated composite plates", *Appl. Math. Model.*, **39**(9), 2489-2508.
Malekzadeh, P. and Monajjemzadeh, S.M. (2013), "Dynamic response of functionally graded plates in thermal environment under moving load", *Compos. Part B: Eng.*, **45**(1), 1521-1533.
Mantari, J.L. and Guedes Soares, C. (2012), "Bending analysis of thick exponentially graded plates using a new trigonometric higher order shear deformation theory", *Compos. Struct.*, **94**(6), 1991-2000.
Mantari, J.L. and Granados, E.V. (2015), "Dynamic analysis of functionally graded plates using a novel FSDT", *Compos. Part B*, **75**, 148-155.
Meksi, R., Benyoucef, S., Mahmoudi, A., Tounsi, A., Adda Bedia, E.A. and Mahmoud, S.R. (2018), "An analytical solution for bending, buckling and vibration responses of FGM sandwich plates", *J. Sandw. Struct. Mater.*, 1099636217698443.
Menasria, A., Bouhadra, A., Tounsi, A., Bousahla, A.A. and Mahmoud, S.R. (2017), "A new and simple HSDT for thermal stability analysis of FG sandwich plates", *Steel Compos. Struct.*, **25**(2), 157-175.
Merdaci, S., Tounsi, A. and Bakora, A. (2016), "A novel four variable refined plate theory for laminated composite plates", *Steel Compos. Struct.*, **22**(4), 713-732.
Mouffoki, A., Adda Bedia, E.A., Houari, M.S.A., Tounsi, A., Mahmoud, S.R. (2017), "Vibration analysis of nonlocal advanced nanobeams in hygro-thermal environment using a new two-unknown trigonometric shear deformation beam theory", *Smart Struct. Syst.*, **20**(3), 369-383.
Mousavi, S.M. and Tahani, M. (2012), "Analytical solution for bending of moderately thick radially functionally graded sector plates with general boundary conditions using multi-term extended Kantorovich method", *Compos. Part B: Eng.*, **43**(3), 1405-1416.
Neves, A.M.A., Ferreira, A.J.M., Carrera, E., Roque, C.M.C.. Cinefra, M., Jorge, R.M.N. and Soares, C.M.M. (2012), "A quasi-3D sinusoidal shear deformation theory for the static and free vibration analysis of functionally graded plates", *Compos. Part B Eng.*, **43**, 711-725.
Karama, M., Afaq, K.S. and Mistou, S. (2003), "Mechanical behaviour of laminated composite beam by the new multi-layered laminated composite structures model with transverse shear stress continuity", *J. Sol. Struct.*, **40**(6), 1525-1546.
Kar, V.R. and Panda, S.K. (2015), "Nonlinear flexural vibration of shear deformable functionally graded spherical shell panel", *Steel Compos. Struct.*, **18**(3), 693-709.
Krishna Murty, A.V. (1987), "Flexure of composite plates", *Compos. Struct.*, **7**(3), 161-177.
Kar, V.R., Panda, S.K. and Mahapatra, T.R. (2016), "Thermal buckling behaviour of shear deformable functionally graded single/doubly curved shell panel with TD and TID properties", *Adv. Mater. Res.*, **5**(4), 205-221.
Koizumi, M. (1997), "FGM activities in Japan", *Compos. Part B: Eng.*, **28**(1-2), 1-4.
Kolahchi, R., Hosseini, H. and Esmailpour, M. (2016a), "Differential cubature and quadrature-bolotin methods for

dynamic stability of embedded piezoelectric nanoplates based on visco-nonlocal-piezoelasticity theories", *Compos. Struct.*, **157**, 174-186.

Kolahchi, R., Safari, M. and Esmailpour, M. (2016b), "Dynamic stability analysis of temperature-dependent functionally graded CNT-reinforced visco-plates resting on orthotropic elastomeric medium", *Compos. Struct.*, **150**, 255-265.

Kolahchi, R., Zarei, M.S., Hajmohammad, M.H. and Nouri, A. (2017a), "Wave propagation of embedded viscoelastic FG-CNT-reinforced sandwich plates integrated with sensor and actuator based on refined zigzag theory", *J. Mech. Sci.*, **130**, 534-545.

Kolahchi, R., Zarei, M.S., Hajmohammad, M.H. and Oskouei, A.N. (2017b), "Visco-nonlocal-refined zigzag theories for dynamic buckling of laminated nanoplates using differential cubature-bolotin methods", *Thin-Wall. Struct.*, **113**, 162-169.

Kolahchi, R., Keshtegar, B. and Fakhar, M.H. (2017c), "Optimization of dynamic buckling for sandwich nanocomposite plates with sensor and actuator layer based on sinusoidal-visco-piezoelasticity theories using grey wolf algorithm", *J. Sandw. Struct. Mater.*, In Press.

Kolahchi, R. and Cheraghbak, A. (2017), "Agglomeration effects on the dynamic buckling of viscoelastic microplates reinforced with SWCNTs using bolotin method", *Nonlin. Dyn.*, **90**(1), 479-492.

Kolahchi, R. (2017), "A comparative study on the bending, vibration and buckling of viscoelastic sandwich nano-plates based on different nonlocal theories using DC, HDQ and DQ methods", *Aerosp. Sci. Technol.*, **66**, 235-248.

Madani, H., Hosseini, H. and Shokravi, M. (2016), "Differential cubature method for vibration analysis of embedded FG-CNT-reinforced piezoelectric cylindrical shells subjected to uniform and non-uniform temperature distributions", *Steel Compos. Struct.*, **22**(4), 889-913.

Pradyumna, S. and Bandyopadhyay, J.N. (2008), "Free vibration analysis of functionally graded curved panels using a higher-order finite element formulation", *J. Sound Vibr.*, **318**(1-2), 176-192.

Reddy, J.N. and Phan, N.D. (1985), "Stability and vibration of isotropic, orthotropic and laminated plates according to a higher-order shear deformation theory", *J. Sound Vibr.*, **98**.

Reddy, J.N. (2000), "Analysis of functionally graded plates", *J. Numer. Meth. Eng.*, **47**(1-3), 663-684.

Sekkal, M., Fahsi, B., Tounsi, A. and Mahmoud, S.R. (2017a), "A new quasi-3D HSDT for buckling and vibration of FG plate", *Struct. Eng. Mech.*, **64**(6), 737-749.

Sekkal, M., Fahsi, B., Tounsi, A., Mahmoud, S.R. (2017b), "A novel and simple higher order shear deformation theory for stability and vibration of functionally graded sandwich plate", *Steel Compos. Struct.*, **25**(4), 389-401.

Senthilnathan, N.R., Chow, S.T., Lee, K.H. and Lim, S.P. (1987), "Buckling of shear-deformable plates", *AIAA J.*, **25**(9), 1268-1271.

Shahrjerdi, A., Mustapha, F., Bayat, M., Sapuan, S.M., Zahari, R. and Shahzamanian, M.M. (2011), "Natural frequency of F.G. rectangular plate by shear deformation theory", *Mater. Sci. Eng.*, **17**.

Shimpi, R.P., Arya, H. and Naik, N.K. (2003), "A higher order displacement model for the plate analysis", *J. Reinf. Plast. Comp.*, **18**(22), 1667-1688.

Shokravi, M. (2017a), "Buckling analysis of embedded laminated plates with agglomerated CNT-reinforced composite layers using FSDT and DQM", *Geomech. Eng.*, **12**(2), 327-346.

Shokravi, M. (2017b), "Vibration analysis of silica nanoparticles-reinforced concrete beams considering agglomeration effects", *Comput. Concrete*, **19**(3), 333-338.

Shokravi, M. (2017c), "Dynamic pull-in and pull-out analysis of viscoelastic nanoplates under electrostatic and casimir forces via sinusoidal shear deformation theory", *Microelectr. Reliab.*, **71**, 17-28.

Shokravi, M. (2017d), "Buckling of sandwich plates with FG-CNT-reinforced layers resting on orthotropic elastic medium using Reddy plate theory", *Steel Compos. Struct.*, **23**(6), 623-631.

Srinivas, S., Joga, C.V. and Rao, A.K. (1970a), "Bending, vibration and buckling of simply supported thick orthotropic rectangular plate and laminates", *J. Sol. Struct.*, **6**, 1463-1481.

Srinivas, S., Joga, C.V. and Rao, A.K. (1970b), "Exact analysis for vibration of simply supported homogeneous and laminated thick rectangular plates", *J. Sound Vibr.*, **12**, 187-199.

Soldatos, K.P. (1992), "A transverse shear deformation theory for homogeneous monoclinic plates", *Acta Mech.*, **94**(3), 195-220.

Taibi, F.Z., Benyoucef, S., Tounsi, A., Bachir Bouiadjra, R., Adda Bedia, E.A. and Mahmoud, S.R. (2015), "A simple shear deformation theory for thermo-mechanical behaviour of functionally graded sandwich plates on elastic foundations", *J. Sandw. Struct. Mater.*, **17**(2), 99 - 129.

Thai, H.T. and Kim, S.E. (2013), "A size-dependent functionally graded Reddy plate model based on a modified couple stress theory", *Compos. Part B: Eng.*, **45**(1), 1636-1645.

Tounsi, A., Houari, M.S.A., Benyoucef, S. and Adda Bedia, E.A. (2013), "A refined trigonometric shear deformation theory for thermoelastic bending of functionally graded sandwich plates", *Aerosp. Sci. Technol.*, **24**, 209-220.

Touratier, M. (1991), "An efficient standard plate theory", *J. Eng. Sci.*, **29**(8), 901-916.

Whitney, J.M. and Pagano, N.J. (1970), "Shear deformation in heterogeneous anisotropic plates", *J. Appl. Mech.*, **37**, 1031-1036.

Zamanian, M., Kolahchi, R. and Bidgoli, M.R. (2017), "Agglomeration effects on the buckling behaviour of embedded concrete columns reinforced with SiO_2 nano-particles", *Wind Struct.*, **24**(1), 43-57.

Zarei, M.S., Kolahchi, R., Hajmohammad, M.H. and Maleki, M. (2017), "Seismic response of underwater fluid-conveying concrete pipes reinforced with SiO_2 nanoparticles and fiber reinforced polymer (FRP) layer", *Soil Dyn. Earthq. Eng.*, **103**, 76-85.

Zemri, A., Houari, M.S.A., Bousahla, A.A. and Tounsi, A. (2015), "A mechanical response of functionally graded nanoscale beam: an assessment of a refined nonlocal shear deformation theory beam theory", *Struct. Eng. Mech.*, **54**(4), 693-710.

Zenkour, A.M. (2006), "Generalized shear deformation theory for bending analysis of functionally graded plates", *Appl. Math. Model.*, **30**(1), 67-84.

Zidi, M., Tounsi, A., Houari M.S.A., Adda Bedia, E.A. and Anwar Bég, O. (2014), "Bending analysis of FGM plates under hygro-thermo-mechanical loading using a four variable refined plate theory", *Aerosp. Sci. Technol.*, **34**, 24-34.

Zidi, M., Houari, M.S.A., Tounsi, A., Bessaim, A. and Mahmoud, S.R. (2017), "A novel simple two-unknown hyperbolic shear deformation theory for functionally graded beams", *Struct. Eng. Mech.*, **64**(2), 145-153.

Zine, A., Tounsi, A., Draiche, K., Sekkal, M. and Mahmoud, S.R. (2018), "A novel higher-order shear deformation theory for bending and free vibration analysis of isotropic and multilayered plates and shells", *Steel Compos. Struct.*, **26**(2), 125-137.

CC